# Demonstration of Vernier effect tuning in tunable twin-guide laser diodes

R. Todt, Th. Jacke, R. Laroy, G. Morthier and M.-C. Amann

**Abstract:** Device and tuning characteristics of superstructure grating tunable twin-guide (SSG-TTG) laser diodes are presented. The devices are based on the distributed feedback (DFB) TTG laser, but comprise sampled or superstructure gratings in order to utilise Vernier effect tuning to extend the tuning range to potentially several tens of nanometres. In contrast to most other existing monolithic widely tunable semiconductor lasers, this device requires only two tuning currents. The first tuning characteristics show distinct regions of high SMSR where continuous wavelength tuning can be carried out. These regions of high SMSR are spaced in agreement with theoretical predictions that are based on the superstructure grating design. Hence, our observations clearly demonstrate Vernier effect tuning for the first time in a TTG-type laser diode.

## 1 Introduction

Wavelength-agile single-frequency laser diodes have received considerable attention in recent years, since they are generally being regarded as essential components for various telecommunication applications [1]. In the short run, they are most likely to be used as backups for conventional fixed-wavelength transmitters. With modern wavelength division multiplexing (WDM) communication systems operating on a large number of wavelength channels, a correspondingly large number of fixed-wavelength transmitters has to be kept in stock as spares, which is quite costly. However, with a widely tunable laser being able to operate on any of the available channels, inventory costs can be reduced significantly. Moreover, in the long run they are expected to become enabling key components for future generations of optical networks. They can be used to introduce new functionalities, like packet switching and wavelength conversion, and thereby make optical networks more flexible. Besides these telecommunications applications, tunable laser diodes are also highly attractive light sources for gas sensing applications [2] as well as for fibre Bragg grating (FBG) based sensor devices [3].

Apart from the fact that a variety of monolithic widely tunable lasers has been presented so far (an overview is given in [4], and specific laser structures are described in detail in [5–7]) and some of them are even commercially available, practically all of them suffer from certain drawbacks. The most well known one is certainly the elaborate calibration procedure that is usually necessary to define the operation points of each specific device. This is a consequence of the presently employed device structures: all concepts to achieve wide wavelength tuning are based on three or even more tuning currents (and one additional current for the gain section). Hence it is necessary to determine typical device characteristics like emission wavelength, side mode suppression ratio (SMSR), and output power as a function of at least three tuning currents, which is very time consuming and therefore also expensive. Other drawbacks include limited output powers (in the case of (S)SG-DBR lasers) and limited direct modulation capabilities due to rather long device cavities.

An alternative to monolithic widely tunable lasers are DFB laser arrays, offering excellent wavelength stability and easy wavelength control [8]. However, their tuning speed cannot compete with monolithic tunable lasers.

Many of the aforementioned problems of the presently available monolithic widely tunable lasers can be overcome by using DFB-like laser structures. Several potential solutions, which require only two tuning currents for wide wavelength tuning, have been presented in recent years. Kim *et al.* [9] and Ishii *et al.* [10] have investigated structures that contain short alternating active and tuning sections. These structures require complex growth and fabrication technologies. Morthier *et al.* [11] have proposed the so-called sampled or superstructure grating widely tunable twin-guide (S)SG-TTG) laser. It is based on the well-known distributed feedback tunable twin-guide (DFB-TTG) laser diode [12]. By replacing the DFB grating with two sections containing sampled gratings (SG) or superstructure gratings (SSG), the (S)SG-TTG laser diode is capable of Vernier effect tuning to achieve wide wavelength tuning. Owing to its DFB-like structure, a phase tuning section is not necessary and, therefore, only two tuning currents are required to set the emission wavelength. Thus, very efficient device characterisation as well as easier device control seems viable. Moreover, high output power can be expected from optimised devices and there is even potential for direct modulation at high frequencies of 10 GHz or more.

In this paper, we present device characteristics of the first widely tunable SSG-TTG laser diodes. First, in Section 2, the device structure and operation principle will be



*IEE Proceedings* online no. 20045018

doi: 10.1049/ip-opt:20045018

Paper first received 25th June 2004 and in revised form 8th February 2005

R. Todt, Th. Jacke and M.-C. Amann are with the Walter Schottky Institut, Technische Universität München, Am Coulombwall, D-85748 Garching, Germany

R. Laroy and G. Morthier are with the Ghent University – IMEC, Department of Information Technology, Sint-Pietersnieuwstratt 41, B-9000 Gent, Belgium

E-mail: todt@wsi.tum.de

explained. Section 3 will summarise the device fabrication and point out crucial fabrication steps with regard to the device performance. Section 4 will then focus on the lasing and tuning performance of the first devices, and finally conclusions will be drawn in Section 5.

## 2 Operation principle

A schematic drawing of an SSG-TTG laser diode is shown in Fig. 1. The TTG laser consists basically of two transversally integrated *p-n* heterojunctions that form the active and tuning regions. They are electrically decoupled by an *n*-InP separation layer and, therefore, can be biased independently from each other. Additionally, the *n*-InP separation layer is also the common *n*-contact of the active and tuning regions, which are contacted laterally. Current confinement in this structure is accomplished by laterally surrounding the active and tuning regions by *p-n* homojunctions (formed of high band-gap material). From an optical point of view, the device forms (in lateral and transverse directions) a singlemode waveguide. In order to ensure also longitudinal singlemode operation, a diffraction grating is employed. Hence, the emission wavelength is determined by the grating period and the effective refractive index of the waveguide. Tuning is now brought about by changing the effective index, either by carrier injection into the tuning region or by heating the device. While tuning due to carrier injection is commonly preferred over electro-thermal tuning, it is important to note that either of these methods are suitable to achieve tuning and have been successfully employed [12].

In order to overcome the tuning limit that is imposed by the maximum achievable refractive index change ($\Delta\lambda/\lambda = \Delta n/n \sim 0.01$), the Vernier effect is being employed in the widely tunable TTG. The tuning region is split up into two parts of approximately equal length and either SGs or SSGs

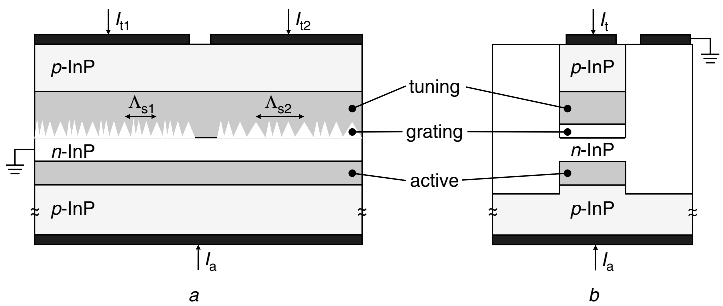


**Fig. 1** *Schematic drawing of SSG-TTG laser diode*

*a* Longitudinal cross-section
*b* Transverse/lateral cross-section

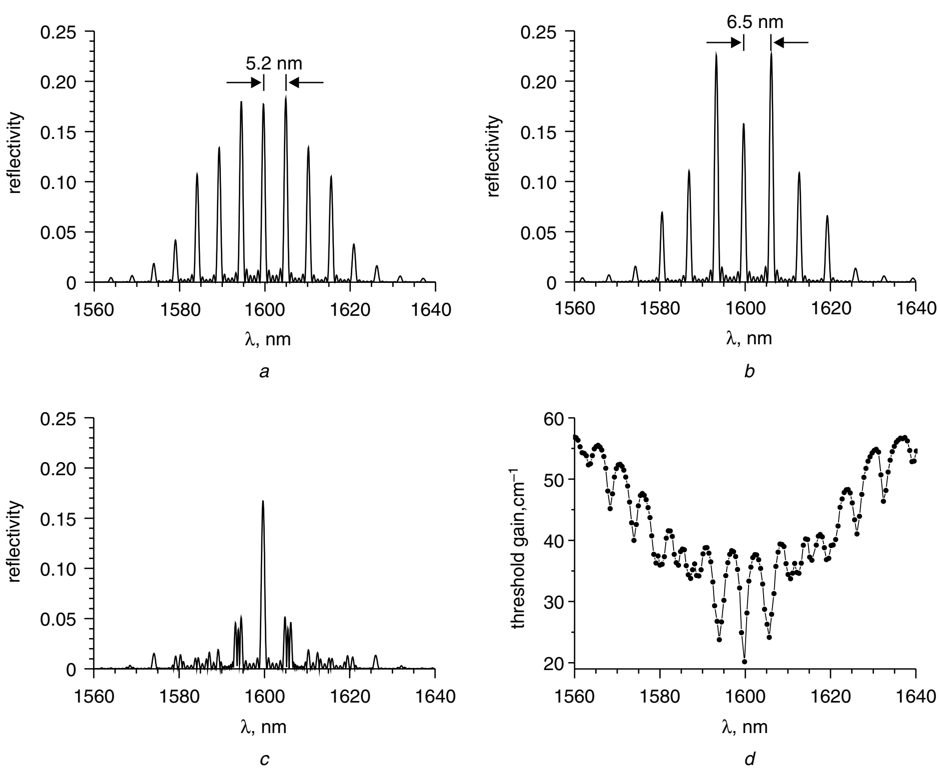


**Fig. 2** *Calculated reflection spectra and cavity modes of SSG-TTG laser diode*

*a* Reflection spectrum of tuning section 2
*b* Reflection spectrum of tuning section 1
*c* Product of both reflection spectra
*d* Cavity modes

are used as reflectors that provide comb-like reflection spectra [13, 14]. The gratings are designed in such a way, that the central Bragg wavelength is the same in both tuning sections. However, the reflection peak spacing, which is determined by the sampling or superstructure period $\Lambda_s$, is chosen slightly different.

Figures 2*a* and *b* show examples of calculated reflection spectra of two SSGs that are similar to the ones employed in our devices. Lasing will occur at the wavelength where reflection peaks of both tuning sections line up best, which is at a wavelength of 1600 nm in the present example (Fig. 2*c*). Although considering reflection spectra is helpful in understanding the device principle, it is actually necessary to investigate the location of the cavity modes since a TTG laser is a DFB-like structure. Hence, also the same considerations regarding facet reflections and phase shifts apply to the SSG-TTG laser as for the DFB laser. Figure 2*d* shows the cavity modes of a widely tunable TTG, assuming a $\pi$ phase shift between the tuning sections. As can be clearly seen, a high degree of side mode suppression can be obtained owing to the large difference in threshold gain of the main mode and the strongest side mode.

Tuning can be carried out in two different ways. By varying both tuning currents simultaneously such that the overlapping pair of reflection peaks keeps lined up, continuous tuning is obtained. Alternatively, larger wavelength jumps are achieved by keeping one tuning current fixed and changing the other one. In this case only little tuning is necessary to line up another pair of reflection peaks. This so-called Vernier effect tuning is crucial to extend the tuning range of the TTG laser.

## 3 Fabrication

The device is based on the GaInAsP/InP material system For the material growth, four chemical beam epitaxy (CBE) growth steps have been employed. SEM images of a finished SSG-TTG laser are shown in Fig. 3.

The fabrication starts with the growth of the active region and the *n*-InP separation layer. A strained layer multi-quantum well (SL-MQW) with photoluminescence (PL) peak at 1.56 μm is used as the active region. The MQW consists of five 7 nm-thick GaInAsP wells that are separated by 9 nm-thick barrier layers (GaInAsP with $\lambda_g = 1.24$ μm). The MQW is embedded in a separate confinement heterostructure (SCH) that consists of GaInAsP layers with $\lambda_g = 1.24$ μm and $\lambda_g = 1.1$ μm.

Subsequently, gratings are defined by e-beam lithography and are etched $\sim 40$ nm deep into the 80 nm-thick *n*-InP separation layer. The superstructure periods ($\Lambda_{s1}, \Lambda_{s2}$) were chosen such that a reflection peak spacing of 5.2 and 6.5 nm was obtained. The gratings are then overgrown with a 180 nm-thick bulk GaInAsP tuning layer ($\lambda_g = 1.35$ μm). Stripe mesas are defined in a dielectric mask and transferred into the semiconductor by reactive ion etching (RIE), resulting in 1.5 μm-broad and 0.7 μm-deep mesas. The mesas, which are still capped by the dielectric mask, are then laterally embedded with *n*-InP ($N_D \sim 2 \times 10^{18}\,\mathrm{cm}^{-3}$) by a selective area growth step. After that, the *p*-cladding is grown in another selective area growth step. Finally passivation and metallisations are applied to finish the device. After fabrication, 600 μm-long devices have been cleaved and the facets were AR-coated by a quarter-wave $Al_2O_3$ film.

Crucial for the performance of the device is the quality of the numerous regrowth interfaces. These coincide also with the *p-n* interfaces of the *p-n* homojunctions (indicated as dashed white lines in Fig. 3), which are relevant for the current confinement in this structure. Hence any surface contamination or crystal damage leads to strongly increased recombination at the InP *p-n* homojunctions. This essentially deteriorates the current confinement of the device structure. Thus, carrier injection into the active or tuning region becomes less efficient and, additionally, heat is generated in close proximity to the buried ridge. At this point it should be noted that tuning due to carrier injection decreases the emission wavelength whereas electrothermal tuning increases the emission wavelength. Since these two tuning mechanisms counteract, it solely depends on their ratio whether the device shows an increase or decrease of the emission wavelength with increasing tuning current. Analysis of test structures has shown that severe leakage currents are present in our devices and, hence, electrothermal tuning dominates.

Further investigations have shown that the poor interface quality, which causes the leakage currents, is mainly an issue of devices that are overgrown in CBE. Although good interface quality can also be obtained using CBE, reproducibility appears to be the main challenge. First experiments, using metal-organic vapour phase epitaxy (MOVPE) for the overgrowth steps, suggest that interfaces of high quality are regularly obtained by MOVPE and adequate current confinement should be achievable in future device generations.

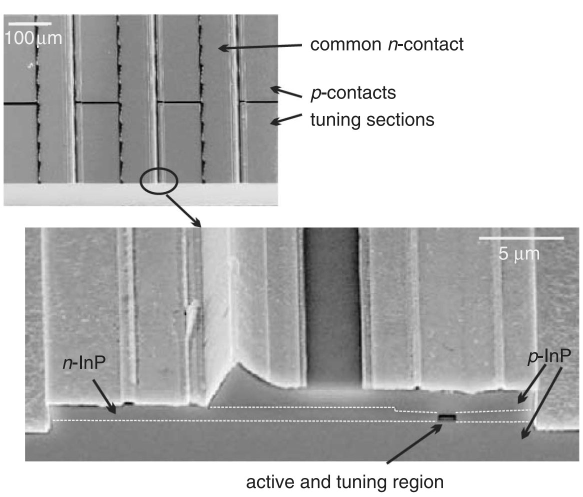


**Fig. 3** *SEM images of finished SSG-TTG laser chip*
Dashed white lines in lower image indicate position of InP *p-n* homojunctions

## 4 Lasing and tuning characteristics

In the following, data from a 1.5 μm-broad and 600 μm-long device will be presented For characterisation, the laser was mounted junction-side up on a Cu heatsink, which was kept at a temperature of 20°C during all measurements.

Light-current and voltage-current characteristics of an SSG-TTG laser are shown in Fig. 4. The lasing threshold is reached at a current of 18 mA and a voltage of 0.89 V. During this measurement, the tuning sections were left unbiased. A maximum fibre-coupled output power of 6 mW is obtained at an active region current of 100 mA. The saturation of the output power at currents above 50 mA is due to the onset of leakage currents over the *p-n* homojunction. Figures 5–7 show the behaviour of the emission wavelength, the SMSR and the fibre-coupled output power as functions of the two tuning currents. During the measurement of these tuning characteristics, the active

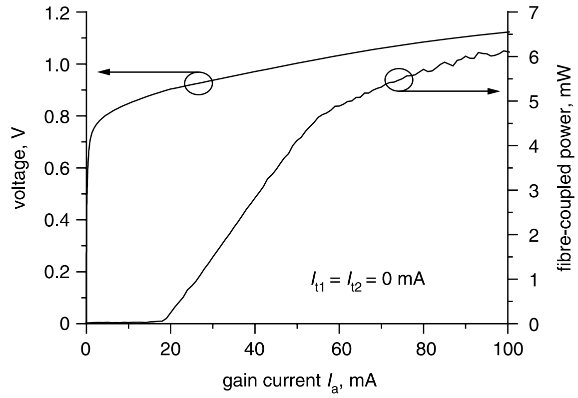


**Fig. 4** *L-I and V-I characteristics*

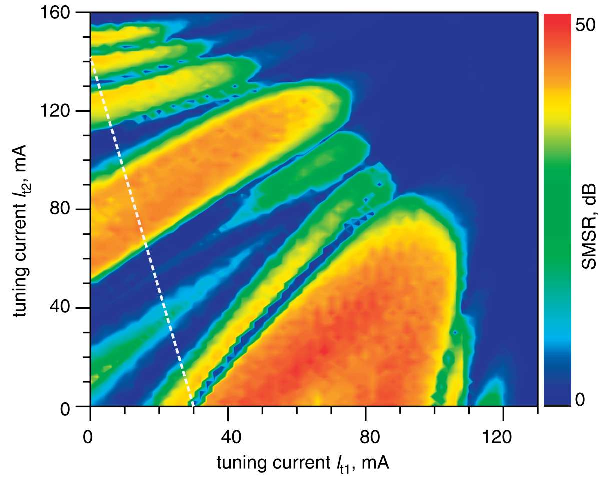


**Fig. 6** *Tuning behaviour of SMSR*

The regions of high SMSR (i.e. >30 dB) characterise the various supermodes. The dashed line indicates the tuning curve shown in Fig. 8

region current was kept constant at 60 mA. As can be seen from the plot of the emission wavelength, the central reflection peaks of the superstructure gratings are located at around 1590–1600 nm. Compared to the PL peak of the active region (~1560 nm), an unintentional detuning of the grating reflection spectra towards longer wavelength becomes apparent. Furthermore it can be seen that there are several bands, also referred to as supermodes (which can be more easily recognised by identifying the regions of high SMSR), where continuous tuning can be carried out by varying both tuning currents simultaneously. Within these supermodes, the emission wavelength is shifting towards longer wavelength, which is characteristic for the electro-thermal tuning. In contrast, by increasing only one tuning current distinct wavelength jumps occur, because another pair of reflection peaks becomes lined up. In the case of increasing $I_{t2}$, these jumps take place towards shorter wavelength. The magnitude of these wavelength jumps is about 5.0 nm, which is in close agreement with the theoretically predicted 5.2 nm. Alternatively, by increasing only $I_{t1}$, jumps towards longer wavelength would be expected. However, starting from the supermode at around 1600 nm, which already requires some tuning of $I_{t1}$, first a rather large wavelength jump of 13.2 nm towards shorter wavelength is observed. From there onward, jumps towards longer wavelength are observed as expected. Presumably owing to the strong detuning of the grating and the gain maximum, there is not enough gain available to support lasing at wavelengths even longer than 1600 nm. Therefore, a jump occurs to the short wavelength side of the superstructure grating and then the Vernier effect tuning proceeds towards longer wavelength again.

It is also worth noting that stable singlemode operation requires some tuning. Since a phase shift has not been incorporated in the present devices, the modal spectrum is degenerate in the untuned and symmetrically tuned case. Hence, some tuning current has to be applied in order to lift the degeneracy and obtain stable singlemode operation.

The evolution of the emission wavelength and the SMSR along the tuning curve that is indicated in Figs. 5 and 6 as a dashed line is shown Fig. 8. Distinct wavelength plateaus with high SMSR (~40 dB) are clearly observable. These are separated by the aforementioned 5.0 nm spacing. The irregular behaviour between $I_{t2} = 20$ and 60 mA is within the region, where both tuning regions are more or less equally tuned, resulting in a degenerate modal spectrum that prevents proper singlemode emission at 1594 nm.

Typically, the SMSR (Fig. 6) is significantly above 30 dB in regions where continuous tuning is carried out and two reflection peaks are perfectly lined up. The highest SMSR observed is around 47 dB. The various supermodes are separated by regions with low SMSR, which is the position where another pair of reflections peaks becomes lined up and large wavelength jumps occur. A typical optical emission spectrum at an operation point with moderate

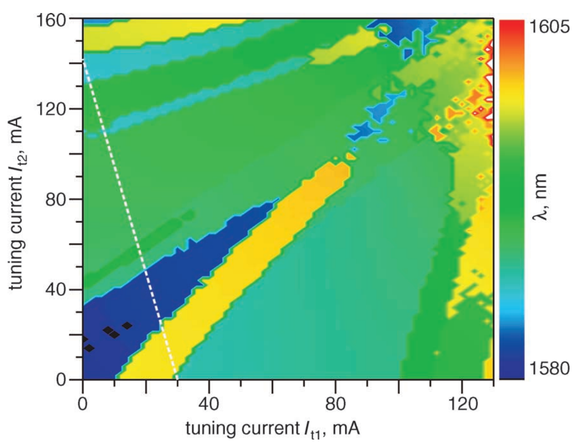


**Fig. 5** *Tuning behaviour of emission wavelength*

The various supermodes can be most easily recognised by identifying the regions of high SMSR in Fig. 6. The dashed line indicates the tuning curve shown in Fig. 8

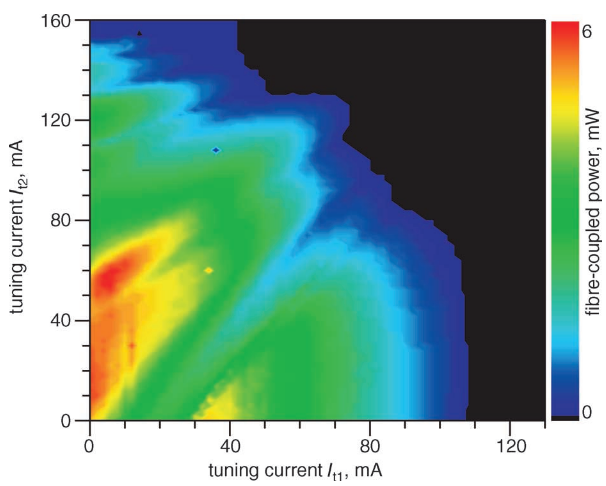


**Fig. 7** *Tuning behaviour of output power*

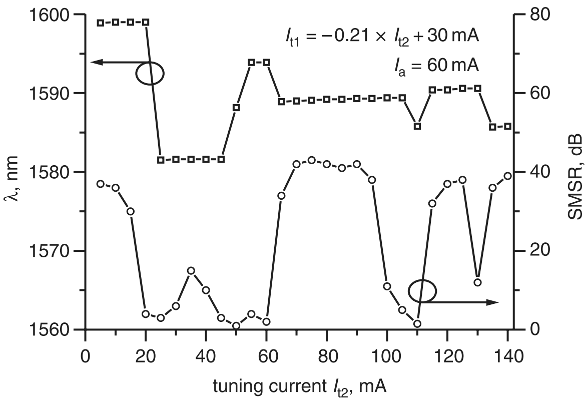


**Fig. 8** *Behaviour of emission wavelength and SMSR along exemplary tuning curve indicated in Figs. 5 and 6*

SMSR is shown in Fig. 9. The spectrum clearly shows that the SMSR is limited by reflections from the non-vanishing overlap of neighbouring reflection peaks and not by adjacent cavity modes. This situation is typical for widely tunable lasers that employ the Vernier effect.

The variation of the fibre-coupled power during tuning is shown in Fig. 7. Highest values are around 5.6 mW. As can be expected, the output power decreases with increasing tuning currents. The regions of perfectly lined up reflections peak not only shows best SMSR, but also the output power is highest there. The maximum output power is comparable to prior reports on DFB-TTG laser diodes [12, 15]. However, one should note that substantially higher output power levels above 20 mW are achievable with optimised devices [15].

The regions, where the SSG-TTG laser operates single-moded (i.e. SMSR > 30 dB) and has an output power in excess of 0.5 mW, make up about 6.5 nm. Figure 10 shows the SMSR as well as both tuning currents $I_{t1}$ and $I_{t2}$ against wavelength. This graph has been created using the dataset of Figs. 5–7. It can be observed how the wavelength increases with increasing tuning currents within each supermode. The largest wavelength change within one supermode, which also corresponds to the maximum continuous tuning range of the device, amounts to ~ 2 nm. The fact that the emission wavelength can be tuned continuously without observing any strong decrease in the SMSR over a wavelength range that is significantly larger than the cavity mode spacing (~ 0.6 nm), confirms the theoretical prediction that a phase tuning section is not necessary. Different supermodes are most easily recognised by a different ratio of $I_{t1}$ and $I_{t2}$. It is worth noting that the tuning currents vary regularly within

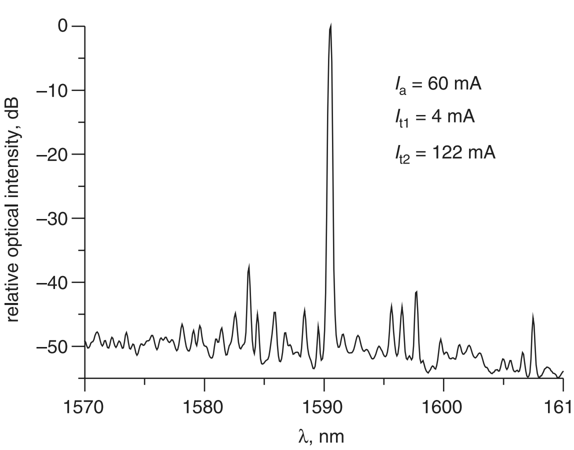


**Fig. 9** *Typical optical emission spectrum*

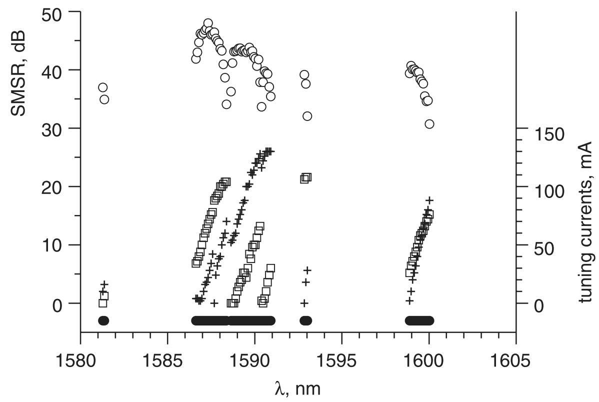


**Fig. 10** *SMSR (○) and tuning currents $I_{t1}$(□) and $I_{t2}$(+) against emission wavelength*

The solid black lines at the bottom are shown in order to make the accessible wavelength range more readily identifiable

each supermode. The lines at the bottom of the graph are shown in order to indicate the overall accessible wavelength range of 6.5 nm. A further extension of the overall tuning range to 8.5 nm is achieved by increasing the gain current from 60 mA to 100 mA.

The overall tuning range is substantially smaller than that of other Vernier tunable lasers. It is, nevertheless, significantly larger than its continues tuning range, which is only tunable by about 2 nm and, hence, a tuning enhancement by a factor of 4 is obtained. The small continuous tuning range is severely limiting the overall tuning performance and is mainly due to the inefficient electrothermal tuning of the device. Significant improvements can be expected by improving the quality of the regrowth interfaces as discussed in the preceding Section. A continuous tuning range of 6–7 nm can be expected from devices with good current confinement. Along with the tuning enhancement by means of the Vernier effect that has been demonstrated, an overall tuning range of above 30 nm can be achieved.

## 5 Conclusions

We have presented experimental results from the first SSG-TTG laser diodes. The tuning characteristics show distinct regions of high SMSR, where continuous wavelength tuning can be carried out. These supermodes are spaced in agreement with theoretical predictions that are based on the superstructure grating design. Hence, the observations clearly demonstrate Vernier effect tuning for the first time in a TTG laser diode. The continuous tuning range of ~2 nm was enhanced by a factor of ~4. However, owing to the small continuous tuning range of the devices, the overall tuning range is significantly smaller than the one of state-of-the-art widely tunable lasers and improvements in the device fabrication, i.e. of the growth interface quality, are required to extend the tuning range to several tens of nanometers. In agreement with theoretical predictions, a phase tuning section, commonly required in longitudinally integrated devices in order to adjust the cavity mode position, was demonstrated not to be necessary in the SSG-TTG laser diode. Therefore, only two tuning currents are required to achieve wide wavelength tuning.

## 6 Acknowledgments

This work has been funded by the European Union via the Information Society Technologies (IST) project

IST-2000-28244 ‘NEWTON’. R. Laroy acknowledges the Institute for the Promotion of Innovation by Science and Technology in Flanders (IWT) for a specialisation grant. The authors wish to thank J. Grottenthaler for providing technical assistance during epitaxial growth and device fabrication.

## 7 References

1 Coldren, L.A.: ‘Monolithic tunable diode lasers’, *IEEE J. Sel. Top. Quantum Electron.*, 2000, **6**, (6), pp. 988–998
2 Upschulte, B.L., Sonnenfroh, D.M., and Allen, M.G.: ‘Measurements of CO, $CO_2$, $H_2O$ in room-temperature and combustion gases by use of broadly current-tuned multisection InGaAsP diode laser’, *Appl. Opt.*, 1999, **38**, (9), pp. 1506–1512
3 Chan, C.C., Jin, W., Ho, H.L., and Demokan, M.S.: ‘Performance analysis of a time-division-multiplexed fiber Bragg grating sensor array by use of a tunable laser source’, *IEEE J. Sel. Top. Quantum Electron.*, 2000, **6**, (5), pp. 741–749
4 Amann, M.-C., and Buus, J.: ‘Tunable laser diodes’ (Artech House, Norwood, USA, 1998)
5 Jayaraman, V., Heimbuch, M.E., Coldren, L.A., and DenBaars, S.P.: ‘Widely tunable continuous-wave InGaAsP/InP sampled grating lasers’, *Electron. Lett.*, 1994, **30**, (18), pp. 1492–1494
6 Wesström, J.-O., Hammerfeldt, S., Buus, J., Silijan, R., Laroy, R., and de Vries, H.: ‘Design of a widely tunable modulated grating Y-branch laser using the additive vernier effect for improved super-mode selection’. Proc. of 18th Int. Semiconductor Laser Conf. (ISLC), Garmisch, Germany, 2002
7 Reid, D.J.C., Robbins, D.J., Ward, A.J., Whitbread, N.D., Williams, P.J., Busico, G., Carter, A.C., Wood, A.K., Carr, N., Asplin, J.C., Kearley, M.Q., Hunt, W.J., Brambley, D.R., and Rawsthorne, J.R.: ‘A novel broadband DBR laser for DWDM networks with simplified quasi-digital wavelength selection’. Proc. of Optical Fiber Communication (OFC) Conf., Anaheim, USA, 2002
8 Hatakeyama, H., Naniwae, K., Kudo, K., Suzuki, N., Sudo, S., Ae, S., Muroya, Y., Yashiki, K., Satoh, K., Morimoto, T., Mori, K., and Sasaki, T.: ‘Wavelength-selectable microarray light sources for S-, C-, and L-band WDM systems’, *IEEE Photonics Technol. Lett.*, 2003, **15**, (7), pp. 903–905
9 Kim, S., Chung, Y., Oh, S.-H., and Park, M.-H.: ‘Design and analysis of widely tunable sampled grating DFB laser diode integrated with sampled grating distributed Bragg reflector’, *IEEE Photonics Technol. Lett.*, 2004, **16**, (1), pp. 15–17
10 Ishii, H., Kondo, Y., Kano, F., and Yoshikuni, Y.: ‘A tunable distributed amplification DFB laser diode (TDA-DFB-LD)’, *IEEE Photonics Technol. Lett.*, 1998, **10**, (1), pp. 30–32
11 Morthier, G., Moeyersoon, B., and Baets, R.: ‘A λ/4-shifted sampled or superstructure grating widely tunable twin-guide laser’, *IEEE Photonics Technol. Lett.*, 2001, **13**, (10), pp. 1052–1054
12 Wolf, T., Illek, S., Rieger, J., Borchert, B., and Amann, M.-C.: ‘Tunable twin-guide (TTG) distributed feedback (DFB) laser with over 10 nm continuous tuning range’, *Electron. Lett.*, 1993, **29**, (24), pp. 2124–2125
13 Jayaraman, V., Chuang, Z.-M., and Coldren, L.A.: ‘Theory, design, and performance of extended tuning range semiconductor lasers with sampled gratings’, *IEEE J. Quantum Electron.*, 1993, **29**, (6), pp. 1824–1834
14 Ishii, H., Tohmori, Y., Tamamura, T., and Yoshikuni, Y.: ‘Super-structure grating (SSG) for broadly tunable DBR lasers’, *IEEE Photonics Technol. Lett.*, **4**, (4), pp. 393–395
15 Schmidt, B., Illek, S., Gessner, R., and Amann, M.-C.: ‘Design and realization of a buried-heterostructure tunable-twin-guide laser diode with electrical blocking regions’, *IEEE J. Quantum Electron.*, 1999, **35**, (5), pp. 794–802